Polymer 50 (2009) 2819–2825

Contents lists available at ScienceDirect

Polymer

journal homepage: www.elsevier.com/locate/polymer

Preparation of molecularly imprinted polymer microspheres via reversible addition–fragmentation chain transfer precipitation polymerization

Guoqing Pan, Baiyi Zu, Xianzhi Guo, Ying Zhang, Chenxi Li, Huiqi Zhang*

Key Laboratory of Functional Polymer Materials (Nankai University), Ministry of Education, Department of Chemistry, Nankai University, Tianjin 300071, PR China

ARTICLE INFO

Article history:
Received 14 November 2008
Received in revised form
20 April 2009
Accepted 22 April 2009
Available online 3 May 2009

Keywords:
Molecular imprinting
Reversible addition–fragmentation chain transfer (RAFT) polymerization
Precipitation polymerization

ABSTRACT

The first combined use of reversible addition–fragmentation chain transfer (RAFT) polymerization and precipitation polymerization in the molecular imprinting field is described. The new polymerization technique, namely *RAFT precipitation polymerization* (RAFTPP), provides MIP microspheres with obvious molecular imprinting effects towards the template, fast template binding process and an appreciable selectivity over structurally related compounds, while only irregular MIP aggregates were obtained via traditional radical precipitation polymerization (TRPP) under similar reaction conditions. The MIP microspheres prepared via RAFTPP have proven to show improved binding capacity, larger binding constant and apparent maximum number for high-affinity sites, and significantly higher high-affinity binding site density in comparison with the MIP prepared via TRPP.

1. Introduction

Molecular imprinting technique is a simple and efficient method to introduce specific molecular recognition sites into a polymer matrix. The resulting molecularly imprinted polymers (MIPs) can show not only an affinity and a selectivity approaching those of antibody–antigen systems but also favorable mechanical, thermal and chemical stability, which make MIPs very promising candidates for many applications, including their use for separation and isolation purposes, as antibody mimics (biomimetic assays and sensors), as enzyme mimics (biomimetic catalysis), in organic synthesis and in drug development [1–5].

A typical molecular imprinting system usually contains a template molecule, a functional monomer, a crosslinking monomer and a suitable solvent, where the functional monomer interacts with the template via non-covalent interactions (hydrogen bonds, ionic and hydrophobic interactions) to form a complex prior to the crosslinking reaction. After polymerization, the template is removed from the obtained polymer network, leading to molecularly imprinted binding sites complementary to the shape, size and functionality of the template. MIPs are normally prepared by free radical polymerization mechanism, whose widespread use can be ascribed to its tolerance for a wide range of functional groups in the monomers and templates as well as its mild reaction conditions. However, traditional radical polymerization processes are usually rather difficult to control with regard to chain propagation and termination, which normally result in polymer networks with heterogeneous structures [6]. The presence of heterogeneity within the network structures of the MIPs could have significant impact on the binding sites inside the networks, which might be responsible for some of the inherent drawbacks of the MIPs such as the broad binding site heterogeneity and the relatively low affinity. Therefore, it can be envisioned that the preparation of MIPs with homogeneous network structures will be of significant importance both for better understanding the structure–property relationship of the MIPs and for obtaining MIPs with improved binding properties. In this respect, controlled/"living" radical polymerization techniques (CRPs) are perfectly suited for this purpose. It has been well understood that the structural heterogeneity in the polymer networks generated by traditional radical polymerization is due to the mismatch between the rapid chain growth and slow chain relaxation, which leads to the reduced reactivity of the pendant vinyl group and/or various cyclization reactions and the formation of heterogeneous polymer networks distributed with highly crosslinked microdomains [6]. In sharp contrast, CRPs are thermodynamically controlled processes with negligible chain termination and a more constant and much slower rate for the polymer chain growth, which significantly improve the match in the chain growth and chain relaxation rates and thus lead to homogeneous polymer networks with a narrow distribution of the network chain length and a much lower crosslinking density in comparison

* Corresponding author. Tel.: +86 2223507193.
E-mail address: zhanghuiqi@nankai.edu.cn (H. Zhang).

0032-3861/$ – see front matter © 2009 Elsevier Ltd. All rights reserved.
doi:10.1016/j.polymer.2009.04.053

with that of the highly crosslinked microdomains in the heterogeneous polymer networks (note that the crosslinking density in the MIPs prepared via CRPs should be still high enough to be able to stabilize the binding sites due to the use of large amounts of crosslinkers). So far, many different polymer networks with homogeneous structures have been prepared via CRPs [6–9].

Among the CRPs developed so far, reversible addition–fragmentation chain transfer (RAFT) polymerization has proven to be one of the most versatile systems because of its applicability to a wide range of monomers (most monomers polymerizable by free radical methods) and its mild reaction conditions [10]. The controllability of the RAFT polymerization lies in the use of a reversible chain transfer agent (CTA, normally a dithioester) and the resulting fast and dynamic equilibrium between active species (propagating radicals) and dormant species (thiocarbonylthio-terminated chains) (Scheme 1a). The polymers generated via RAFT polymerization generally contain a dithioester end group, which makes their further chain modification possible. RAFT polymerization has so far been mainly utilized to prepare well-defined linear polymers. Very recently, RAFT polymerization has also been used for the preparation of cosslinked ones including MIPs [11–14] and other homogeneous polymer networks [9]. Titirici and Sellergren reported the successful grafting of cross-linked MIP films on the surfaces of mesoporous silica beads through RAFT polymerization [11]. Yang and Wang's group described a general protocol for preparing surface-imprinted core–shell nanoparticles via RAFT polymerization using RAFT agent functionalized silica nanoparticles as the chain transfer agent [12]. Van Houten and coworkers prepared europium(III) containing insoluble or soluble MIPs for the luminescent sensing of organophosphates by RAFT polymerization or by a combination of RAFT polymerization and ring-closing metathesis [13,14]. So far, RAFT polymerization has shown great potential in preparing MIPs with improved properties (e.g., faster binding kinetics [11]) and tailor-made structures [11,12], to our knowledge, however, its application in molecular imprinting is still rather limited. Therefore, it should be of great importance to extend the application of RAFT polymerization to the synthesis of MIPs with different formats in order to show its versatility.

Precipitation polymerization has proven very versatile for preparing MIP micro-/sub-microspheres because of its easy operation and no need for any surfactant or stabilizer [15–18], but only traditional radical precipitation polymerization (TRPP) has been used for this purpose up to now. Recently, a combined use of RAFT polymerization and precipitation polymerization (namely RAFT precipitation polymerization (RAFTPP)) has been reported for the preparation of polymer microspheres [19–21], where the introduction of the RAFT mechanism into the precipitation polymerization allowed the easy preparation of functional polymer microspheres with reactive dithioester groups on their surfaces, thus making them highly useful for further surface modification either by reinitiation via RAFT polymerization [19,20] or by using standard organic procedures (e.g., Diels–Alder chemistry) [21]. In the present communication, we report on the application of RAFTPP in the molecular imprinting field for the preparation of functional MIP microspheres (Scheme 1b). The chemical structures, particle size and morphology, template rebinding properties, surface properties and binding selectivity of the obtained MIP

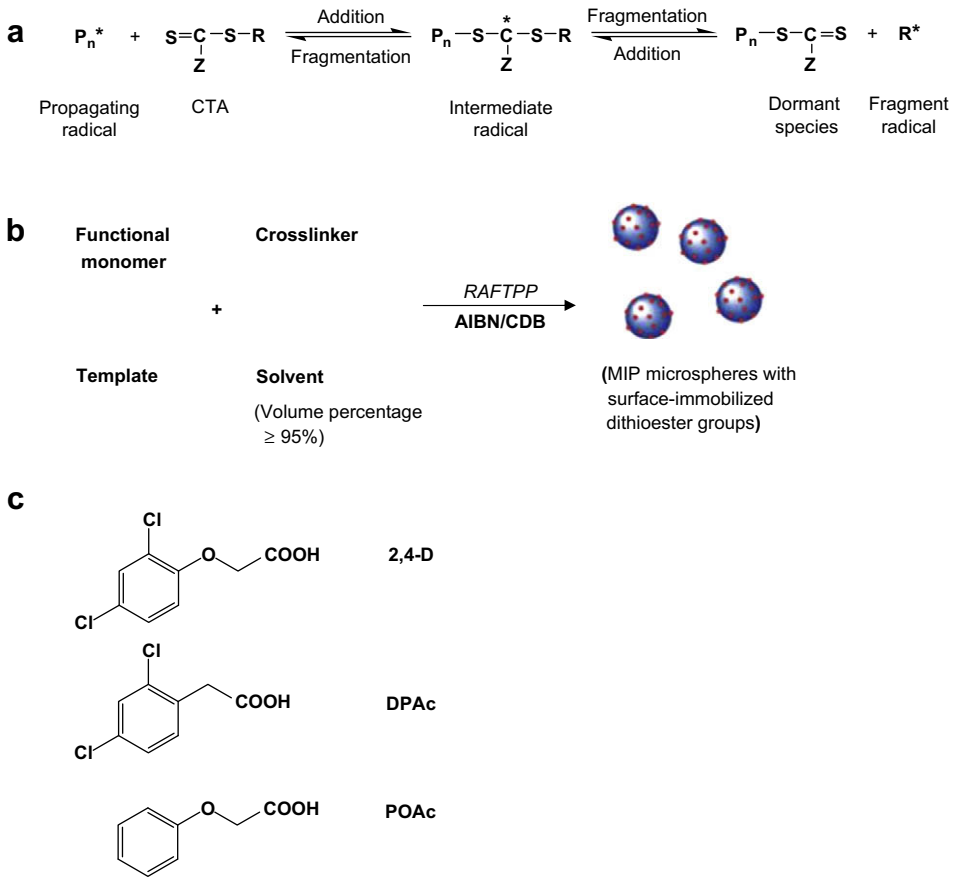

Scheme 1. The mechanism of the RAFT polymerization (a), the schematic representation of the RAFTPP process (b) and chemical structures of 2,4-D and its related compounds (c).

microspheres were characterized, and they were also compared with those of the MIP particles prepared via TRPP.

2. Experimental section

2.1. Materials

4-Vinylpyridine (4-VP, Alfa Aesar, 96%) and ethylene glycol dimethacrylate (EGDMA, Alfa Aesar, 98%) were purified by distillation under vacuum. Azobisisobutyronitrile (AIBN, Chemical Plant of Nankai University, analytical grade (AR)) was recrystallized from ethanol. Cumyl dithiobenzate (CDB) was prepared following a literature procedure [22]. Methanol (Jiangtian Chemical Ltd., China, AR) was distilled prior to use. 2,4-Dichlorophenoxyacetic acid (2,4-D, Alfa Aesar, 98%), 2,4-dichlorophenylacetic acid (DPAc, Acros, 99%) and phenoxyacetic acid (POAc, Acros, 98+%) were used as-received and their chemical structures are presented in Scheme 1c.

2.2. Preparation of the MIP/NIP by RAFTPP

The 2,4-D imprinted polymer was prepared via RAFTPP according to the following procedure: 4-VP (0.2102 g, 1.9992 mmol), 2,4-D (0.1108 g, 0.5013 mmol) and a mixture of methanol and water (4/1 v/v, 160 mL) was added into a one-neck round-bottom flask (250 mL). After 30 min of stirring at room temperature, a clear solution was obtained, to which EGDMA (1.9825 g, 10.0010 mmol), AIBN (0.0181 g, 0.1102 mmol) and CDB (0.0612 g, 0.2247 mmol) were added. The reaction mixture was purged with argon for 30 min and sealed. The flask was then immersed into a thermostated oil bath at 60 °C for 24 h. The generated polymer particles were collected by filtration, purified through Soxhlet extraction with methanol/acetic acid (9/1 v/v, 48 h) and methanol (24 h) and then dried at 40 °C under vacuum for 48 h to provide an MIP with a light pink color (yield: 80%).

The non-imprinted polymer (NIP, light pink color) was prepared and purified under the identical conditions except that the template was omitted (yield: 85%).

2.3. Preparation of the MIP/NIP by TRPP

The MIP/NIP was prepared by TRPP following a similar procedure as RAFTPP except that CDB was omitted. White MIP and NIP were obtained with their yields being 88 and 90%, respectively.

2.4. Characterization of chemical structures, particle size and morphology, and surface properties of the MIPs/NIPs

Fourier Transform Infrared (FT-IR) spectra of the MIPs were obtained using a Nicolet Magna-560 FT-IR spectrometer.

The particle size and size distribution of the MIPs/NIPs were determined with a scanning electron microscope (SEM, Shimadzu SS-550 for Fig. 1a and b and Hitachi S-3500N for Fig. 1c and d). All of the SEM size data reflect the averages about 100 particles each, which are calculated by the following formula:

$$U = D_w/D_n; \quad D_n = \sum_{i=1}^{k} n_i D_i / \sum_{i=1}^{k} n_i;$$

$$D_w = \sum_{i=1}^{k} n_i D_i^4 / \sum_{i=1}^{k} n_i D_i^3$$

where U is the polydispersity index, D_n the number-average diameter, D_w the weight-average diameter, k the total number of the measured particles, n_i the particle number of the determined microspheres, and D_i the particle diameters of the determined microspheres.

Surface property analysis was performed by nitrogen sorption porosimetry on a TriStar3000 Surface Area and Porosimetry

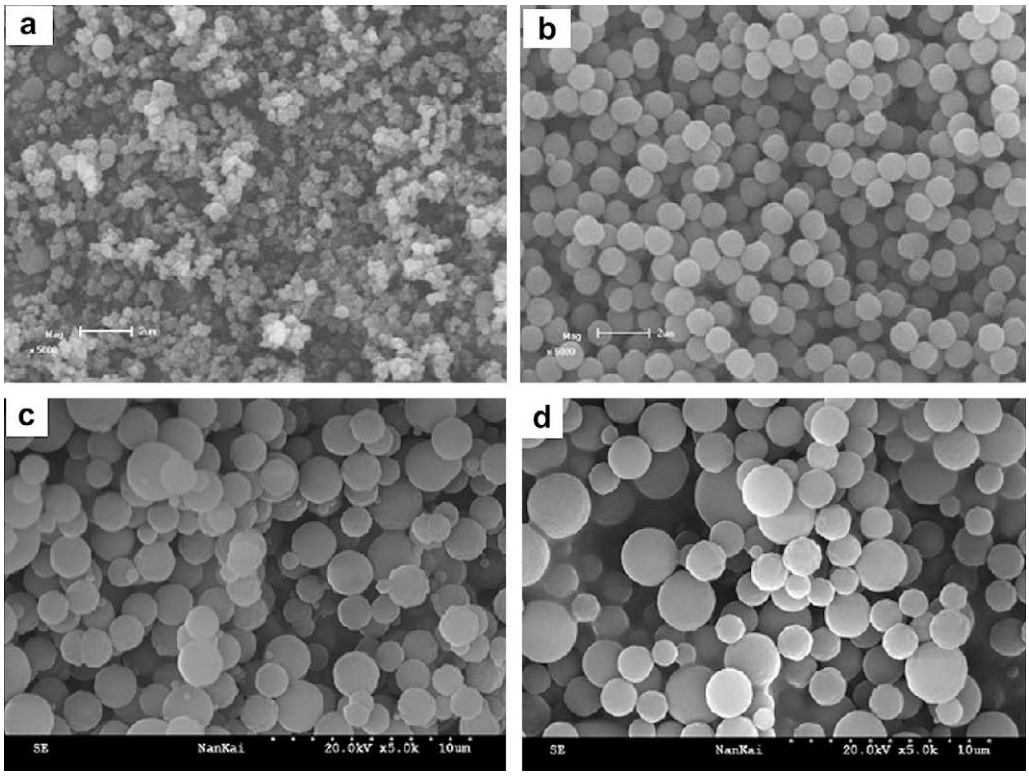

Fig. 1. Scanning electron micrographs of the MIPs (a, c) and NIPs (b, d) prepared via TRPP (a, b) and RAFTPP (c, d), respectively.

Analyzer (America Micromeritics Instrument Corp). Prior to the measurements, the MIPs/NIPs were degassed at 100 °C under high vacuum for 10 h. The surface areas (S) of the MIP/NIP microspheres were then evaluated by using the Brunauer–Emett–Teller (BET) method, while their specific pore volumes (V_p) and the average pore diameters (d_p) were evaluated using the Barrett, Joyner and Halenda (BJH) theory.

2.5. HPLC measurements and evaluation

The concentrations of the template and its related compounds were quantified with a high-performance liquid chromatography (HPLC, Scientific System Inc., USA) with a UV–vis detector. The wavelength used for the determination of 2,4-D, DPAc and POAc was 284, 272 and 270 nm, respectively. A mixture of methanol and 0.5% aqueous solution of acetic acid (4/1 v/v) was used as the mobile phase at a flow rate of 1 mL/min.

2.5.1. Binding experiments

Binding kinetics of the template molecule 2,4-D with the MIPs/NIPs prepared via different synthetic approaches was evaluated by batch adsorption experiments, where 10 mg of MIPs/NIPs were incubated with a solution of 2,4-D in a mixture of methanol and water (4/1 v/v, 1 mL, 0.08 mM) at 23 °C for different times. After centrifugation, the amounts of the template remaining in the supernatants (expressed as F) were determined by HPLC and those bound to the MIPs/NIPs (B) can thus be obtained by subtracting F from the initial template concentration.

Equilibrium binding experiments were performed by incubating a 2,4-D solution in a mixture of methanol and water (4/1 v/v, 1 mL, 0.08 mM) with different amounts of MIPs/NIPs at 23 °C for 16 h. The amounts of the template bound to the MIPs/NIPs were then quantified with HPLC.

Binding isotherms of the MIPs were studied with Scatchard analysis: MIP particles (10 mg) were incubated with a series of 2,4-D solutions (in a mixture of methanol and water: 4/1 v/v, $C = 0.04$–1.0 mM, 1 mL) at 23 °C for 16 h. After centrifugation, the amounts of the template bound to the MIPs (B) were determined by HPLC. The Scatchard equation used is $B/F = (N_{max} - B)K_a$, where K_a and N_{max} represent the binding association constant and apparent maximum number of the binding sites, respectively.

2.5.2. Selectivity evaluation

The binding selectivity of the MIPs was evaluated by measuring their rebinding capacities towards 2,4-D and its structurally related compounds (DPAc and POAc): 10 mg of MIPs were incubated with 1 mL of 2,4-D or its related compound solution in methanol/water (4/1 v/v, $C = 0.08$ mM) at 23 °C for 6 h and the amounts of 2,4-D or the related compounds bound to the MIPs were quantified by HPLC. The selectivity values (%) of the MIPs were obtained by determining the amount of the bound related compound (per unit weight of MIP) relative to that of the bound template.

All the above binding analyses were performed in duplicate and the mean values were used.

3. Results and discussion

Over the past several years, we have been working in the field of molecular imprinting [5,23,24] and CRP [25,26]. In this contribution, we are aiming to combine the above two fields together and will mainly focus on two aspects, i.e., to check whether RAFTPP can be used to prepare MIP microspheres as a new polymerization technique for molecular imprinting and whether the resulting MIPs have some improved binding properties in comparison with those prepared via TRPP.

3.1. Synthesis of MIPs/NIPs via RAFTPP and TRPP

Since the MIPs have been mostly prepared via non-covalent molecular imprinting technique nowadays due to its flexibility in preparation and its versatility in generating MIPs with high specificity and fast rebinding kinetics, a model non-covalent molecular imprinting system was chosen here to show the proof-of-principle, which utilized 2,4-D, 4-VP, EGDMA and a mixture of methanol and water (4/1 v/v) as the template, functional monomer, crosslinker and porogenic solvent, respectively, following a similar reactant/solvent combination used in the literature [27]. RAFTPP was then carried out to prepare 2,4-D imprinted polymer microspheres with AIBN as the initiator and CDB as the chain transfer agent (Scheme 1b), where the molar ratio of 2,4-D to 4-VP to EGDMA to AIBN to CDB was 1:4:20:0.22:0.45. For comparison, TRPP was also performed to prepare MIP particles following a similar procedure as RAFTPP except that CDB was omitted. As references, the corresponding NIP particles were also prepared similarly by omitting the template in the reaction systems. Note that all of the above reactants are compatible with both RAFT polymerization and molecular imprinting process and 4-VP can form hydrophobic interactions and ionic bonds with 2,4-D in polar solvents [27]. All the reactions were performed at 60 °C for 24 h in a mixture of methanol and water (4/1 v/v) with its volume percentage larger than 98%. The resulting polymer particles were purified by Soxhlet extraction with methanol/acetic acid (9/1 v/v) and methanol successively, leading to the desired MIPs/NIPs with their yields ranging from 80 to 90%. A suspension solution of the MIP particles prepared via RAFTPP or TRPP (10 mg) in a mixture of methanol and water (4/1 v/v, 1 mL) was then incubated at 23 °C for 16 h. After centrifugation, the concentrations of the template in the supernatants were found to be negligible, suggesting the successful removal of the template from the obtained MIPs. As expected, white MIP/NIP particles were generated via TRPP while light pink MIP/NIP particles were obtained via RAFTPP, indicating the presence of dithioester groups in the MIP/NIP prepared via RAFTPP.

3.2. Characterization of the chemical structures and particle morphology of the MIPs/NIPs

The obtained MIPs were firstly characterized with FT-IR and the results showed that the MIPs prepared via both RAFTPP and TRPP have rather similar IR spectra (Fig. S1 in the Supporting Information). The presence of three significant peaks around 1729 (C=O stretching), 1252 and 1155 cm^{-1} (C–O–C stretching) supports the existence of poly(EGDMA) in the obtained MIPs. The characteristic peaks corresponding to the C=N stretching (1599 and 1558 cm^{-1}) and C=C stretching (1455 cm^{-1}) in the pyridine rings can also be observed in the spectra, revealing that poly(4-VP) is present in the MIPs. Furthermore, the presence of a small peak around 1635 cm^{-1} (corresponding to the C=C stretching mode) demonstrates that less than 100% of bonded EGDMA molecules are crosslinked in the MIPs prepared via both RAFTPP and TRPP [28].

The particle size and morphology of the MIPs/NIPs were then characterized with SEM (Fig. 1). It can be seen clearly that TRPP provided only irregular MIP aggregates while uniform NIP microspheres were obtained under similar reaction conditions (Fig. 1a and b), revealing that the template compound had an important influence on the particle growth during the precipitation polymerization, as observed by others [17]. The number-average diameter (D_n) and polydispersity index (U) of the NIP microspheres are 1.1 μm and 1.02, respectively. In comparison, RAFTPP provided both MIP and NIP microspheres with their D_n values being 1.8 and 2.0 μm, respectively, and their U values being 1.19 and 1.27, respectively (Fig. 1c and d). The above results suggested that the combined use of RAFT polymerization and precipitation

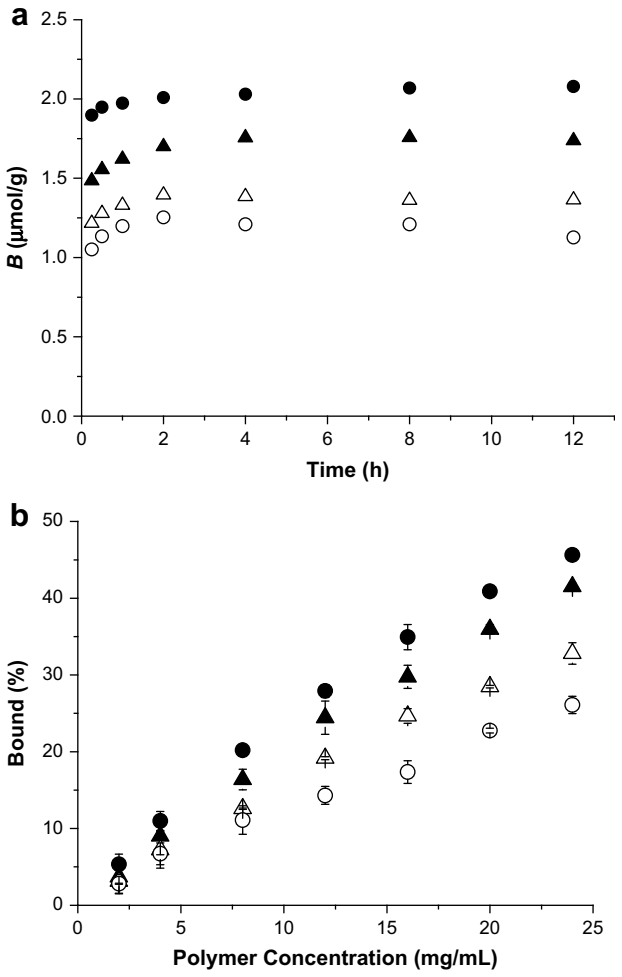

Fig. 2. (a) Binding kinetics of 2,4-D on MIPs (filled symbols) and NIPs (open symbols) prepared via RAFTPP (cycle) and TRPP (triangle), respectively. 10 mg of MIPs/NIPs were incubated with a solution of 2,4-D in methanol/water (4/1 v/v, 1 mL, 0.08 mM) at 23 °C for different times; (b) Equilibrium bindings of 2,4-D in methanol/water (4/1 v/v, 1 mL, $C = 0.08$ mM) on different amounts of MIPs (filled symbols) and NIPs (open symbols) prepared via RAFTPP (cycle) and TRPP (triangle), respectively. The RAFTPP and TRPP were repeated twice in order to show the statistical results.

polymerization could have dramatic influence on the particle size and morphology of the obtained MIPs/NIPs. This may not be surprising given that different polymerization mechanisms are involved in the two systems. The living nature of RAFTPP might somehow influence both the formation of the particle nucleus in the solution and their growth processes [29], thus leading to spherical MIP particles. A detailed study on the mechanism of RAFTPP is under way and the results will be included in a forthcoming paper.

3.3. The binding properties of the MIPs/NIPs

The binding kinetics of the template molecule with the MIPs/NIPs was evaluated by batch adsorption experiments. Fig. 2a shows that all the MIPs/NIPs prepared via both RAFTPP and TRPP reached their binding equilibriums at a time of about 2 h, demonstrating quite fast binding processes. In addition, the MIP prepared via RAFTPP showed higher equilibrium loading capacity than the MIP via TRPP, while the NIP prepared via RAFTPP exhibited lower equilibrium loading capacity than the NIP via TRPP, thus indicating the presence of improved binding properties in the MIP prepared via RAFTPP.

Equilibrium binding experiments were performed to study the template rebinding properties of the MIPs/NIPs. Fig. 2b shows that the MIPs prepared via both RAFTPP and TRPP bound more 2,4-D than their corresponding NIPs. For example, in a mixture of methanol and water (4/1 v/v), while 24 mg of the MIP particles prepared via RAFTPP and TRPP bound 46 and 42% of 2,4-D, respectively, an equivalent amount of the corresponding controls bound only 26 and 33%, respectively, suggesting the presence of selective binding sites in the obtained MIPs. Besides, the MIP prepared via RAFTPP showed higher equilibrium loading capacity than the MIP via TRPP in a wide range of polymer concentrations, while in the meantime the NIP prepared via RAFTPP exhibited lower equilibrium loading capacity than the NIP via TRPP, which fits well with the results obtained in the binding kinetic study (Fig. 2a). It should be mentioned here that both RAFTPP and TRPP were performed twice in order to show the statistical tests, and the quite reproducible results revealed that our results are reliable.

To get more insight into the binding characteristics of the MIPs prepared via different synthetic approaches, they were further studied with Scatchard analysis. The results showed that the Scatchard plots of all the MIPs could be fitted into two straight lines (Fig. S3 in the Supporting Information), suggesting that the binding sites in the MIPs prepared via both RAFTPP and TRPP are heterogeneous and their affinities can be approximated by two binding association constants (K_a) corresponding to the high- and low-affinity sites, as usually observed for the MIPs via non-covalent molecular imprinting approach [30]. We are particularly interested in the high-affinity sites because they are mainly responsible for the specific binding of the MIPs. The K_a and N_{max} values of the high-affinity sites for the MIP prepared via RAFTPP were determined to $3.0 \times 10^4\ M^{-1}$ and 3.5 μmol/g, respectively, and those for the MIP prepared via TRPP were $2.4 \times 10^4\ M^{-1}$ and 2.9 μmol/g, respectively (Table 1). The relatively larger K_a and N_{max} values obtained for the MIP via RAFTPP suggest the presence of higher specific binding in this system.

It is known that the surface properties of the MIPs/NIPs have much influence on their binding properties. Therefore, the MIPs/NIPs were characterized by performing nitrogen adsorption experiments,

Table 1
The isothermal binding parameters, surface properties and binding site densities of the MIP/NIP particles prepared via both RAFTPP and TRPP.

Samples	High-affinity binding sites[a]		Surface properties[b]			High-affinity binding site density[d]
	K_a ($\times M^{-1}\ 10^{-4}$)	N_{max} (μmol/g)	S (m^2/g)	d_p (nm)	V_p (mL/g)	ρ (μmol/m^2)
RAFTPP-MIP	3.0	3.5	2.5	–[c]	–[c]	1.4
RAFTPP-NIP			0.9	–[c]	–[c]	
TRPP-MIP	2.4	2.9	23.2	22	0.0461	0.13
TRPP-NIP			3.2	–[c]	–[c]	

[a] K_a and N_{max} represent the binding association constant and apparent maximum number of the binding sites, respectively; they were obtained from Scatchard analysis.
[b] BET surface areas (S) were determined from nitrogen sorption measurements with the BET model, while the specific pore volumes (V_p) and the average pore diameters (d_p) were evaluated using the BJH theory.
[c] The V_p and d_p values could not be accurately determined in these cases due to their too small surface areas.
[d] High-affinity binding site densities on the surfaces of the MIP particles: $\rho = N_{max}/S$.

and the obtained surface areas (S), the specific pore volumes (V_p), and the average pore diameters (d_p) for the MIPs/NIPs are summarized in Table 1. The surface areas of the MIP and NIP prepared via RAFTPP were determined to be 2.5 and 0.9 m^2/g, respectively, and those of the MIP and NIP prepared via TRPP were 23.2 and 3.2 m^2/g, respectively. In comparison with the irregular MIP aggregates prepared via TRPP (they are actually composed of much smaller particles), both the MIP/NIP spherical particles obtained via RAFTPP and the NIP particles obtained via TRPP showed much smaller surface areas, which might be stemmed from their much larger particle sizes. Based on the surface area values (S) of the MIPs and the previously obtained apparent numbers of binding sites (N_{max}), the high-affinity binding site densities ($\rho = N_{max}/S$) on the surfaces of the MIP particles prepared via RAFTPP and TRPP were calculated to be 1.4 and 0.13 μmol/m^2, respectively, revealing that the MIP microspheres prepared via RAFTPP had a significantly higher high-affinity binding site density than the MIP particles via TRPP. This is likely to be due to the controlled polymerization mechanism of RAFTPP, which leads to increased structural homogeneity and improved stability and integrity of binding sites. Note that the V_p and d_p values could not be accurately determined for both the MIP/NIP prepared via RAFTPP and the NIP prepared via TRPP due to their too small surface areas. Therefore, only the V_p and d_p values for the MIP prepared via TRPP are presented in Table 1. In addition, the pore size distribution of the MIP prepared via TRPP proved to be rather broad (Fig. S4), with its d_p value around 22 nm (Table 1).

The binding selectivity of the MIPs is often determined by comparing the binding of the template with those of its analogues, which affords an indication of the cross-reactivity of the MIPs towards selected molecules. The bindings of the MIPs/NIPs prepared via both RAFTPP and TRPP towards 2,4-D were also compared to two structurally related compounds, DPAc and POAc (Scheme 1c), which have the same functionality (i.e., carboxyl group) but differ either in the distance between the functional group and the benzene ring or in the numbers of substitutents on the benzene ring. As can be seen clearly from Fig. 3a and b, besides binding 2,4-D, the MIPs also adsorbed DPAc and POAc, suggesting the existence of certain cross-binding reactivity. Nevertheless, the MIPs showed significantly lower binding capacities towards DPAc and POAc than towards 2,4-D, thus demonstrating the high selectivity of the MIPs towards 2,4-D (Fig. 3c). It is worth mentioning here that while the presence of certain cross-binding reactivity in the MIPs might be undesirable for such applications as sensors, this could actually be an advantage in sample treatment because a class of template analogues could also be removed or enriched efficiently. Furthermore, it is also worth noting that in comparison with the NIPs prepared via different synthetic approaches, the corresponding MIPs showed relatively higher binding capacities towards not only 2,4-D but also DPAc and POAc. This is understandable because the 2,4-D imprinted cavities in the MIPs could also accommodate DPAc and POAc due to their relatively smaller sizes.

Based on the above results, we can make a close comparison between the MIPs prepared via RAFTPP and TRPP. Previous reports have shown that the application of CRPs in molecular imprinting could have rather different effects on the resulting MIPs. In certain cases, the MIPs prepared via CRPs showed improved binding properties such as faster binding kinetics [11,31], higher binding capacities [31–34] and larger binding association constants [34], while in some other cases, the binding properties of the MIPs prepared via CRPs appeared very similar to those of the MIPs prepared via conventional approaches [35]. In the present study, we found out that RAFTPP could readily provide MIP microspheres while only irregular MIP aggregates were obtained via TRPP under similar reaction conditions, demonstrating the versatility of RAFTPP in the preparation of MIP microspheres. The MIPs prepared via both RAFTPP and TRPP showed obvious molecular imprinting effects towards the template, fast template binding processes and an appreciable selectivity over structurally related compounds. More importantly, the MIP microspheres prepared via RAFTPP have proven to show improved binding capacity, larger binding association constant K_a and apparent maximum number N_{max} for the high-affinity sites, and significantly higher high-affinity binding site density than the MIP via TRPP.

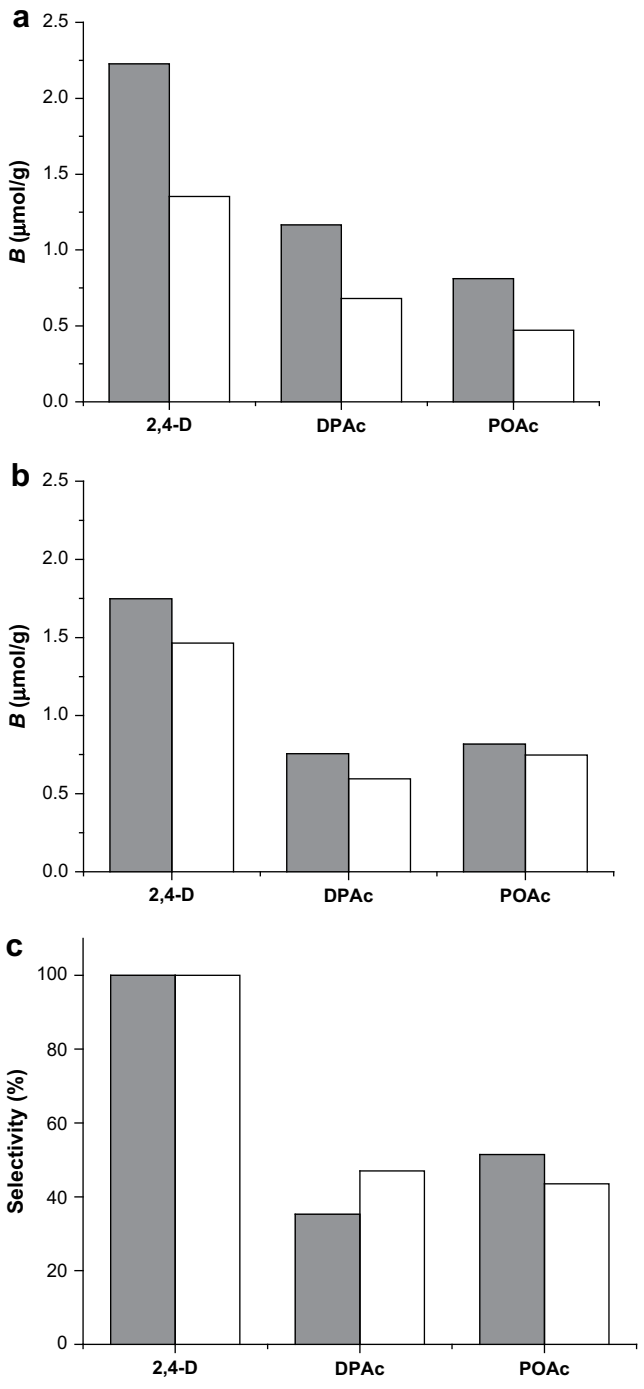

Fig. 3. The bindings of the MIPs (filled columns)/NIPs (open columns) (10 mg) prepared via RAFTPP (a) and TRPP (b) towards 2,4-D, DPAc and POAc in methanol/water (4/1 v/v, $C = 0.08$ mM, 1 mL) at 23 °C for 6 h; (c) Binding selectivity of the MIPs prepared via RAFTPP (filled columns) and TRPP (open columns) towards 2,4-D, DPAc and POAc in methanol/water (4/1 v/v, $C = 0.08$ mM, 1 mL) at 23 °C.

4. Conclusions

We have developed a new approach (i.e., RAFTPP) to prepare functional MIP microspheres which combines RAFT polymerization and precipitation polymerization. The living nature of RAFTPP imparts the obtained MIP microspheres with improved binding capacity, larger K_a and N_{max} values for the high-affinity sites and significantly higher high-affinity binding site density in comparison with the irregular MIP aggregates prepared via TRPP. Considering the general applicability of RAFT polymerization to a wide range of monomers and template molecules, we believe that RAFTPP represents a simple and robust approach to the preparation of functional MIP microspheres with improved binding properties. In addition, the presence of surface-immobilized reactive functional groups on the obtained MIP microspheres allows their further surface modification (eventually leading to their better compatibility with different solvent systems), which makes them highly promising in many practical applications. The work in this direction is currently in progress.

Acknowledgements

We gratefully acknowledge the financial supports from National Natural Science Foundation of China (20744003, 20774044), Natural Science Foundation of Tianjin (06YFJMJC15100), a supporting program for the new century excellent talents (ministry of education) (NCET-07-0462) and the project sponsored by SRF for ROCS, SEM.

Appendix. Supporting Information

FT-IR spectra, template binding isotherms and Scatchard plots of the MIPs prepared via RAFTPP and TRPP, respectively, and the pore size distribution of the MIP prepared via TRPP. Supplementary data associated with this article can be found in the online version, at doi:10.1016/j.polymer.2009.04.053.

References

[1] Wulff G. Angew Chem Int Ed 1995;34:1812–32.
[2] Mosbach K, Ramström O. Biotechnology 1996;14:163–70.
[3] Sellergren B, editor. Molecularly imprinted polymers: man made mimics of antibodies and their applications in analytical chemistry; techniques and instrumentation in analytical chemistry, vol. 23. Amsterdam: Elsevier; 2001.
[4] Haupt K. Chem Commun 2003:171–8.
[5] Zhang H, Ye L, Mosbach K. J Mol Recognit 2006;19:248–59.
[6] Wang AR, Zhu S. Polym Eng Sci 2005;45:720–7.
[7] Huang W, Baker GL, Bruening ML. Angew Chem Int Ed 2001;40:1510–2.
[8] Kanamori K, Hasegawa J, Nakanishi K, Hanada T. Macromolecules 2008; 41:7186–93.
[9] Achilleos M, Legge TM, Perrier S, Patrickios CS. J Polym Sci Part A Polym Chem 2008;46:7556–65.
[10] Moad G, Chiefari J, Chong BYK, Krstina J, Mayadunne RTA, Postma A, et al. Polym Int 2000;49:993–1001.
[11] Titirici MM, Sellergren B. Chem Mater 2006;18:1773–9.
[12] Lu CH, Zhou WH, Han B, Yang HH, Chen X, Wang XR. Anal Chem 2007;79:5457–61.
[13] Southard GE, Van Houten KA, Ott Jr EW, Murray GM. Anal Chim Acta 2007;581:202–7.
[14] Southard GE, Van Houten KA, Murray GM. Macromolecules 2007;40:1395–400.
[15] Ye L, Cormack PAG, Mosbach K. Anal Commun 1999;36:35–8.
[16] Wang J, Cormack PAG, Sherrington DC, Khoshdel E. Angew Chem Int Ed 2003;42:5336–8.
[17] Yoshimatsu K, Reimhult K, Krozer A, Mosbach K, Sode K, Ye L. Anal Chim Acta 2007;584:112–21.
[18] Ye L, Mosbach K. React Funct Polym 2001;48:149–57.
[19] Barner L, Li CE, Hao XJ, Stenzel MH, Barner-Kowollik C, Davis TP. J Polym Sci Part A Polym Chem 2004;42:5067–76.
[20] Joso R, Stenzel MH, Davis TP, Barner-Kowollik C, Barner L. Aust J Chem 2005;58:468–71.
[21] Nebhani L, Sinnwell S, Inglis AJ, Stenzel MH, Barner-Kowollik C, Barner L. Macromol Rapid Commun 2008;29:1431–7.
[22] Le TP, Moad G, Rizzardo E, Thang SH. PCT Int Appl WO 98/01478; Chem Abstr 1998;128:115390.
[23] Zhang H, Verboom W, Reinhoudt DN. Tetrahedron Lett 2001;42:4413–6.
[24] Zhang H, Piacham T, Drew M, Patek M, Mosbach K, Ye L. J Am Chem Soc 2006;128:4178–9.
[25] Zhang H, Klumperman B, Ming W, Fischer H, van der Linde R. Macromolecules 2001;34:6169–73.
[26] Zhang H, Jiang XL, van der Linde R. Polymer 2004;45:1455–66.
[27] Haupt K, Dzgoev A, Mosbach K. Anal Chem 1998;70:628–31.
[28] Koprinarov I, Hitchcock AP, Li WH, Heng YM, Stöver HDH. Macromolecules 2001;34:4424–9.
[29] Li WH, Stöver HDH. J Polym Sci Part A Polym Chem 1998;36:1543–51.
[30] Watabe Y, Hosoya K, Tanaka N, Kubo T, Kondo T, Morita M. J Chromatogr A 2005;1073:363–70.
[31] Wei X, Husson SM. Ind Eng Chem Res 2007;46:2117–24.
[32] Vaughan AD, Sizemore SP, Byrne ME. Polymer 2007;48:74–81.
[33] Wang HJ, Zhou WH, Yin XF, Zhuang ZX, Yang HH, Wang XR. J Am Chem Soc 2006;128:15954–5.
[34] Boonpangrak S, Whitcombe MJ, Prachayasittikul V, Mosbach K, Ye L. Biosens Bioelectron 2006;22:349–54.
[35] Pérez-Moral N, Mayes AG. Macromol Rapid Commun 2007;28:2170–5.